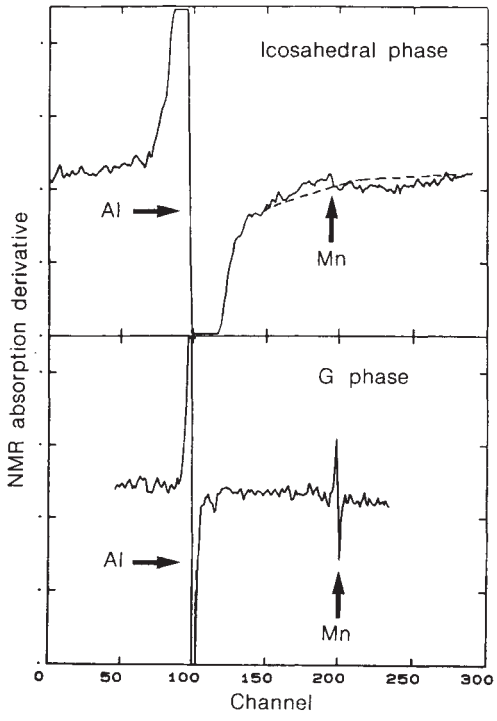

Fig. 1 Comparison of the ^{55}Mn and ^{27}Al nuclear magnetic resonance derivative powder pattern taken at 11.037 MHz at room temperature in icosahedral Al–Mn and in the G phase, $Al_{12}Mn$. The arrows point to the centre of the resonances. In the iAl–Mn, the ^{55}Mn resonance lies in the wings of the ^{27}Al NMR. The Mn resonance in iAl-Mn is revealed by subtracting the continuation of the Al resonance shown by the dashed curve. The ^{27}Al NMR in the G phase is largely masked by the free Al component, but in any case is considerably narrower than the corresponding spectrum for the icosahedral phase. Each channel number is equal to 5.62 Oe.

It is important to distinguish between the symmetry of assemblies of atoms such as crystals or quasicrystals as detected by diffractions, and symmetries of sites occupied by atoms in such assemblies, as detected by probes such as NMR[4,5] and the Mossbauer effect (NGR)[6,7]. (The NMR spectra confirm Mossbauer effect results obtained on the icosahedral phase with some iron atoms substituted for manganese, in which it was assumed that the iron atoms would occupy the same sites as the manganese.) High-symmetry crystals or quasicrystals can occur without any atom occupying a high-symmetry position. For example, the αAl–Mn–Si cubic phase contains[8] icosahedral clusters, with a vacancy at the centre of each. No atom occupies a position of local cubic symmetry. Conversely, highly symmetric clusters often pack into crystals of low symmetry. It is therefore not surprising that the Mn atoms in the Al–Mn icosahedral phase do not occupy positions of high local symmetry. Indeed their local environment seems to be[9] quite similar to that of Mn in the αAl–Mn–Si structure. In a number of recently proposed models[7–14] for the icosahedral phase, the Mn atoms are packed in several ways to produce a structure with long-range icosahedral symmetry, but the nearest-neighbour environment of the Mn atoms is highly unsymmetric. The measured NMR spectrum of the icosahedral phase is consistent with such models. Any model of the Al–Mn icosahedral phase must provide diffraction displaying icosahedral symmetry, but it must also have complex local environments as revealed by the experiments.

Note added in proof: L. Pauling, in commenting on the present work, points out that only 8 of the 195 Mn atoms per cell in his structure lie in positions with cubic point-group symmetry and thus have zero quadrupole broadening. The quadrupole interactions of the other icosahedrally coordinated Mn atoms must be non-zero, but we can estimate that they would be too small to replicate the NMR spectrum of the icosahedral phase. Although the exact equivalence of Pauling's structure based on the packing of Al icosahedra with Mn at their centres to the $NaCd_2$ structure is not clear to us, we have modelled the quadrupole interaction at every site in the $NaCd_2$ structure, and in no case do we find values comparable to those observed. Further distortions of the structure, large enough to fit the data, would render the conceptual representation of the structure by icosahedra invalid.

Received 28 August 1986; accepted 16 January 1987.

1. Pauling, L. *Nature* **317**, 512–514 (1985).
2. Little, K., Raynor, G. V. & Hume-Rothery, W. *J. Inst. Metals* **73**, 83–90 (1946).
3. Schaefer, R. J., Biancaniello, F. S. & Cahn, J. W. *Scr. met.* **20**, 1439–1444 (1986).
4. Rubinstein, M., Stauss, G. H., Phillips, T. E., Moorjani, K. & Bennett, L. H. *J. mater. Res.* **1**, 243–246 (1986).
5. Warren, W. W., Jr, Chen, H. S. & Hauser, J. J. *Phys. Rev.* B**32**, 7614–7616 (1985).
6. Swartzendruber, L. J., Shechtman, D., Bendersky, L. & Cahn, J. W. *Phys. Rev.* B **32**, 1383–1385 (1985).
7. Eibschutz, M., Chen, H. S. & Hauser, J. J. *Phys. Rev. Lett.* **56**, 169–172 (1986).
8. Elser, V. & Henley, C. L. *Phys. Rev. Lett.* **55**, 2883–2886 (1985).
9. Stern, E. A., Ma, Y. & Bouldin, C. E. *Phys. Rev. Lett.* **55**, 2172–2175 (1985).
10. Mackay, A. *Acta crystalogr.* **15**, 916–918 (1962).
11. Audier, M. & Guyot, P. *Phil. Mag.* **53**, L43–L51 (1986).
12. Kuriyama, M., Long, G. G. & Bendersky, L. *Phys. Rev. Lett.* **55**, 849–851 (1985).
13. Watson, R. E. & Weinert, M. *Mater. Sci. Eng.* **79**, 105–109 (1986).
14. Cahn, J. W. & Gratias, D. *J. Phys. Colloq.* C**3**, 415–424 (1986).

Satellite measurements of sea surface cooling during hurricane Gloria

Peter Cornillon*, Lothar Stramma† & James F. Price‡

* Graduate School of Oceanography, University of Rhode Island, Kingston, Rhode Island 02881, USA
† Institut für Meereskunde, Kiel 2300, FRG
‡ Woods Hole Oceanographic Institution, Woods Hole, Massachusetts 02543, USA

Hurricanes and other strong storms can cause important decreases in sea surface temperature by means of vertical mixing within the upper ocean, and by air–sea heat exchange. Here we use satellite-derived infrared images of the western North Atlantic to study sea surface cooling caused by hurricane Gloria (1985). Significant regional variations in sea surface cooling are well correlated with hydrographic conditions. The greatest cooling (up to 5 °C) occurred in slope waters north of the Gulf Stream where the seasonal thermocline is shallowest and most compressed; moderate cooling (up to 3 °C) occurred in the open Sargasso Sea where the thermocline is deeper and more diffused; little or no cooling occurred in shallow coastal waters (bottom depth less than 20 m) which were isothermal before the passage of hurricane Gloria. There is a pronounced right-side asymmetry of sea surface cooling with stronger (by a factor of 4) and more extensive (by a factor of 3) cooling found on the right side of the hurricane track. These qualitative results are consistent with the notion that vertical mixing within the upper ocean is the dominant sea surface cooling mechanism of hurricanes.

Hurricane Gloria (1985) began to form very late in the hurricane season off the Cape Verde Islands[1]. Gloria moved nearly due westward with the trade winds to about the Leeward Islands, and then turned north-west toward the Sargasso Sea. On 25 September the minimum central pressure fell to 919 mbar, making Gloria one of the most powerful Atlantic hurricanes of the past decade. During 26 and 27 September, the central pressure slowly increased as Gloria moved northward at about 7 ms^{-1} over the Sargasso Sea and coastal waters of the north-east United States[1,2] (Fig. 1). Gloria crossed the US coast over Long Island on the afternoon of 27 September. Although considerably weakened by then, Gloria caused substantial property damage in southern New England[2].

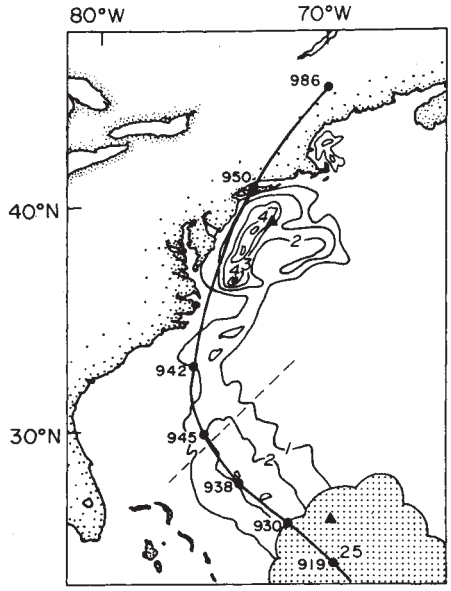

Fig. 1 Magnitude of sea surface cooling observed from satellite infrared images. Contour intervals are 1 °C. The thicker line is the path of hurricane Gloria, which moved to the north; dots are 12 h apart. The number on the right of the southernmost dot along the track refers to the day in September 1985 (at 00:00 GMT). The numbers on the left of the track are hurricane central pressure in mbar. Solid triangles show the location of two expendable bathythermographs (XBTs) that provided the data of Fig. 3, and the dashed diagonal line crossing 30 °N, 75 °W is the SST section of Fig. 4. Stippled area at lower right is clouds.

To see what effects Gloria had on the ocean, we have examined satellite infrared images of the western North Atlantic made by the NOAA-9 Advanced Very High Resolution Radiometer (AVHRR)[3]. The data were decimated to give 4-km resolution, corrected for atmospheric attenuation[4], and scan-angle corrected[5]. Previous studies[4] have shown that the resulting sea surface temperature (SST) data have an absolute accuracy of about 0.5 °C, and a relative error (point-to-point variation) of about 0.2 °C.

A pre-hurricane SST image was formed by compositing night-time images of the western North Atlantic made during 19–23 September (Fig. 2, left). The compositing procedure selected the warmest pixel from the sample in order to reduce the area obscured by cloud cover. (Night-time images were chosen in order to avoid contamination by diurnal warming which can be strong in this region[4,5].) A post-hurricane composite image was formed for the period immediately following the hurricane passage, 27 and 28 September, and by also ensuring that only those regions south of (behind) the hurricane were retained (Fig. 2, right). The post-hurricane data used here are thus less than two days old and nearly synoptic, which helps minimize the unwanted effects of relaxation[6] and distortion by horizontal advection (though advection by the Gulf Stream is apparent as noted below). An estimate of the change in SST caused by the passage of Gloria was obtained by differencing the pre- and post-hurricane SST images (Fig. 2, centre). The same data were also smoothed and contoured to yield Fig. 1. These images are unique, we believe, in showing such a large portion of a hurricane track and in covering a region having a wide range of hydrographic conditions.

The pattern of sea surface cooling appears to be dominated by the response to hurricane Gloria except near the Gulf Stream axis where there is a clear distortion due to horizontal advection. Note the northeastward-extending notch in the cooling contours at the intersection of the hurricane track and the Gulf Stream axis (near 35 °N), and the apparent northeastward displacement of cooled water by as much as 150 km downstream of the Gulf Stream–track intersection (Fig. 1 and Fig. 2, centre).

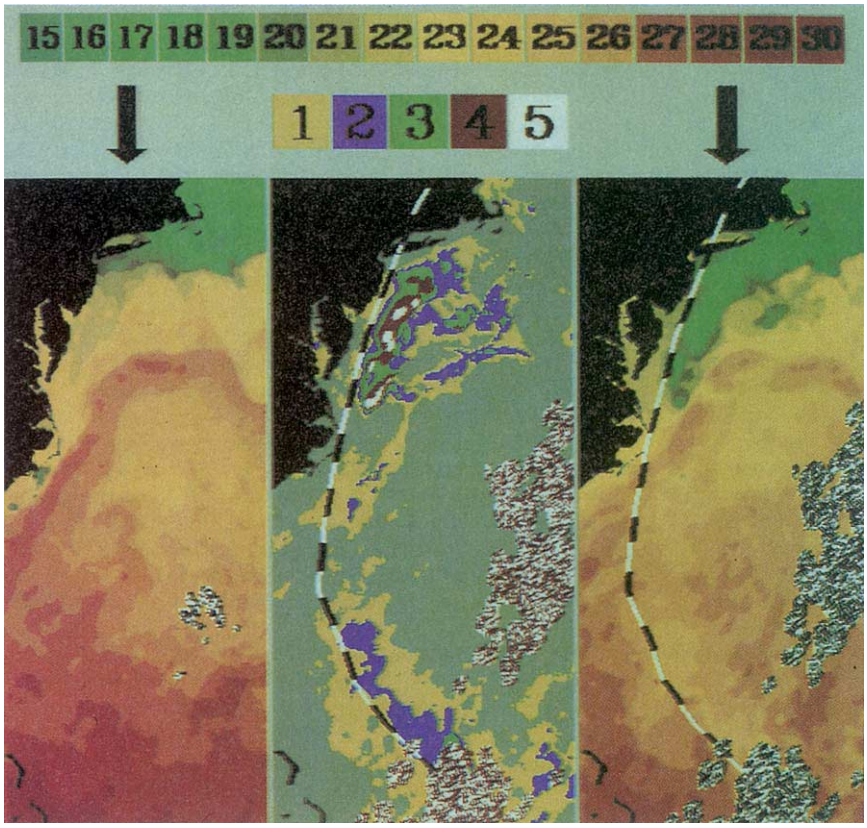

Fig. 2 Composite of pre-hurricane night-time satellite images of the western North Atlantic for 19–23 September 1985 (left). Post-hurricane composite for 27 and 28 September (right). Difference between the pre- and post-hurricane images (centre). Black, masked area is the east coast of the United States from Cape Hatteras to Cape Cod, and stippled areas denote cloud cover. The colour scale at the top of the figure is temperature scale (in °C) for the left and right panels. The second colour scale from the top (range 1–5 °C) applies to the central panel.

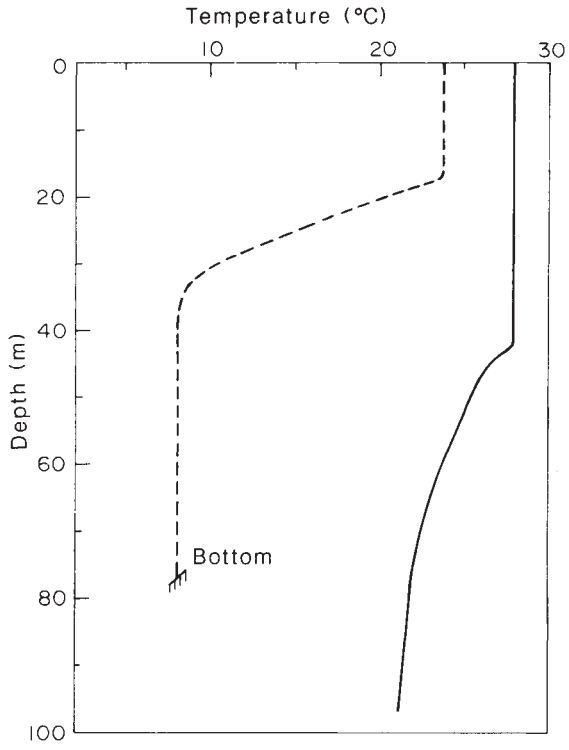

Fig. 3 Pre-hurricane, XBT-derived temperature profiles from slope water north of the Gulf Stream (dashed line, 39 °N, 72 °W, 11 September) and from the southern Sargasso Sea (solid line, 26 °N, 70 °W, 18 September) (see Fig. 1 for locations).

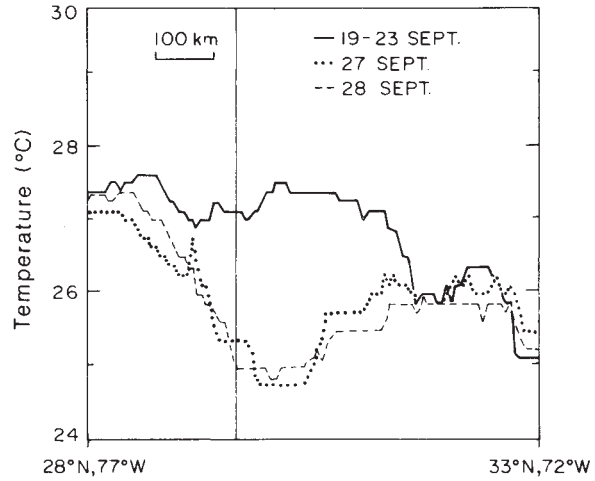

Fig. 4 Satellite-derived 5×5 pixel median-filtered SST sections between 28° N, 77° W and 33° N, 72° W (dashed diagonal line of Fig. 1). A section made through the pre-hurricane composited image is shown by the solid line (19–23 September). Sections made from post-hurricane images are shown by a dotted line (27 September, 07:57 GMT) and by a dashed line (28 September, 07:46 GMT). The thin vertical line to the left of centre marks the intersection with Gloria's track.

These images show a significant regional (or along-track) variation of sea surface cooling which gives useful clues to the mechanism of cooling. Previous model studies have shown that vertical mixing of cooler thermocline waters up into the ocean's surface layer is the dominant mechanism producing sea surface cooling[7,8,9], and that sea surface cooling by a given storm will be greatest where cold thermocline waters are closest to the sea surface. These images support this result as far as regional variations of sea surface cooling appear correlated with hydrographic conditions rather than with hurricane intensity or initial SST. Most notably, hurricane intensity (measured by central pressure, Fig. 1) decreases almost monotonically from south to north along the portion of the hurricane track seen here[1,2]. On the other hand, the strongest sea surface cooling, up to 5 °C, is observed in slope waters to the north of the Gulf Stream where Gloria had already weakened. Along Gloria's track, cold thermocline water is found nearest the sea surface in slope waters where the thermocline is shallow and very compressed compared to the thermocline in the Sargasso Sea (Fig. 3). Thus, hurricane-induced vertical mixing would be expected to reduce the SST more effectively over slope waters than over the Sargasso Sea. However, over shallow coastal waters (bottom depth <20 m; for example, Long Island Sound, Rhode Island Sound, and Nantucket Sound) there was little or no sea surface cooling. By late September these shallow waters are usually already isothermal[10] (Fig. 3), so that further vertical mixing by Gloria could not produce further cooling.

Sea surface cooling shows a striking asymmetry about the track (Fig. 1), with much stronger and more extensive decreases in SST found on the right side of the track compared to the left side (viewing the sea surface from above, and assuming that the hurricane moves toward the top of the figure). This right-side asymmetry has been observed before in conventional, *in situ* data sets[7,11] and in other satellite images[6], though not as clearly. In this case, some of the asymmetry found within coastal waters is attributable to the horizontal variations in hydrographic conditions noted above. Over the open Sargasso Sea this right-side asymmetry of cooling is thought to be a characteristic of the homogeneous ocean's response to a hurricane. (Except in the immediate vicinity of the Gulf Stream, the near-surface currents are on average westward[12,13], so that advection is unlikely to be the cause of the asymmetry.) To quantify the cooling asymmetry, we have sampled the pre- and post-hurricane SST images along a section across the Sargasso Sea (Figs 1 and 4). The maximum sea surface cooling, about 2.6 °C, occurs at distance $R \approx 80$ km to the right of the track. At the same distance to the left of the track, the sea surface cooling is only about 0.6 °C. The ratio $2.6/0.6 \approx 4$ provides one measure of the sea surface cooling asymmetry along this section, and by inspection of Fig. 1, a value characteristic of the cooling throughout the Sargasso Sea. As an alternative measure of asymmetry, we have also calculated the line integral of sea surface cooling from the track out to distances of $4R$ to the right and to the left of the track. The integral cooling to the right of the track is about 550 °C km, and to the left of the track the value is about 180 °C km. These give a ratio of roughly 3. A similar, strong right-side asymmetry of sea surface cooling occurs in numerical models which presume that vertical mixing in the upper ocean is mainly a consequence of shear flow instability of wind-driven currents[7,8].

We thank O. Brown, R. Evans, J. Brown and A. Li at the University of Miami for their assistance with image processing software; D. Evans and R. S. Armstrong for the XBT profiles; and J. Rahn for editorial comments. Supported by contracts N00014-81-0062 (P.C. and L.S.) and N00014-84-C-0134 (J.F.P.) with the US Office of Naval Research.

Received 14 July 1986; accepted 13 January 1987.

1. Case, R. A. & Gerrish, H. P. *Mariners Weath. Log* **30**, 6-11 (1986).
2. DeAngelis, D. *Mariners Weath. Log* **30**, 34-41 (1986).
3. Schwalb, A., *Natn. Oceanogr. Atmos. Admin. tech. Memo NESS 95* (Washington DC, 1978).
4. Stramma, L., Cornillon, P., Weller, R. A., Price, J. F. & Briscoe, M. G. *J. phys. Oceanogr.* **16**, 827-837 (1986).
5. Cornillon, P. & Stramma, L. *J. geophys. Res.* **90**, 11811-11815 (1985).
6. Stramma, L., Cornillon, P. & Price, J. F. *J. geophys. Res.* **91**(C4), 5031-5035 (1986).
7. Price, J. F. *J. phys. Oceanogr.* **11**, 153-175 (1981).
8. Martin, P. J. *J. geophys Res.* **87**, 409-427 (1982).
9. Chang, S. W. & Anthes, R. A. *J. phys. Oceanogr.* **8**, 468-480 (1978).
10. Riley, G. A. *Bull. Bingham oceanogr. Coll.* **15**, 15-46 (1956).
11. Pudov, V. D., Varfolomeyev, A. A. & Fedorov, K. N. *Oceanology* (English transl.) **18**, 142-146 (1978).
12. Beardsley, R. C. & Boicourt, W. C. *Evolution of Physical Oceanography* 198-233 (MIT Press, Cambridge, 1981).
13. Worthington, L. V. *Johns Hopkins oceanogr. Stud.* **6** (1976).